ACS APPLIED MATERIALS & INTERFACES

Research Article

www.acsami.org

Parylene-Coated Ionic Liquid–Carbon Nanotube Actuators for User-Safe Haptic Devices

Grzegorz Bubak,*[,†] David Gendron,[†] Luca Ceseracciu,[‡] Alberto Ansaldo,[†] and Davide Ricci[†]

[†]Istituto Italiano di Tecnologia, Robotics, Brain and Cognitive Sciences Department, Via Morego 30, Genoa, Italy, 16163

[‡]Istituto Italiano di Tecnologia, Smart Materials, Via Morego 30, Genoa, Italy, 16163

Supporting Information

ABSTRACT: Simple fabrication, high power-to-weight and power-to-volume ratios, and the ability to operate in open air at low voltage make the ionic electroactive polymer actuators highly attractive for haptic applications. Whenever a direct tactile stimulation of the skin is involved, electrical and chemical insulation as well as a long-term stability of the actuator are required. Because of its inherent physicochemical properties such as high dielectric strength, resistance to solvents, and biological inactivity, Parylene C meets the requirements for making biocompatible actuators. We have studied the displacement and the generated force of Parylene-coated carbon nanotube actuators as well as the encapsulation quality. A 2 μm coating creates an effective electrical insulation of the actuators without altering the blocking force at frequencies from 50 mHz to 1 Hz. Moreover, the generated strain is preserved at higher frequencies (from 0.5 to 5 Hz). We employed a simple mechanical model to explain the relation between the key parameters—flexural stiffness, displacement, and force—for uncoated and coated actuators. In addition, we demonstrated that our Parylene-coated actuators are not damaged by rinsing in liquid media such as 2-propanol or water. In conclusion, our results indicate that Parylene C encapsulated actuators are safe to touch and can be used in contact with human skin and in biomedical applications in direct contact with tissues and physiological fluids.

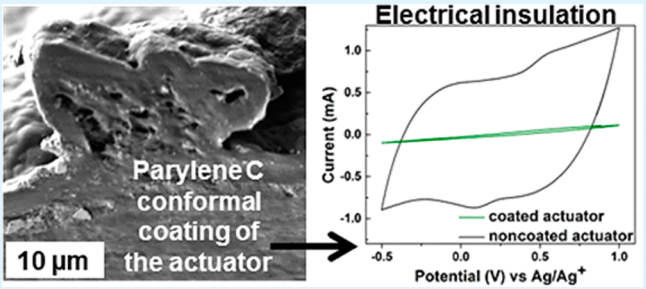

KEYWORDS: *actuators, carbon nanotubes, ionic liquid, Parylene coating, composite materials*

1. INTRODUCTION

Actuators are the key part of many devices and machines that we use everyday. Conventional actuators found in commercial products are usually robust, heavy, rigid, noisy, and often expensive. In recent years, ionic electroactive polymer (iEAP) actuators have drawn great attention[1] due to their interesting properties: they are lightweight, resilient, noiseless, compliant, and can be operated at low-voltage.[2,3] These devices generate strain and force in response to an applied voltage.[4,5] Among them, actuators based on an ionic liquid–carbon nanotube composite[6]—also called bucky gel[7]—are particularly attractive as they can operate at low voltage in air and do not require water or propylene carbonate based electrolytes that could evaporate with time. The bucky gel is made by a vigorous mixing of carbon nanotubes (CNTs) (both single-walled[8] or multiwalled[9] may be used) with an imidazolium-based ionic liquid and a supporting polymer (usually polyvinylidene difluoride, PVDF, or its copolymer hexafluoropropylene, PVDF-HFP) dissolved in *N,N*-dimethylacetamide.[10] Once casted and dried, this gel can be used as a flexible electrode film. In 2005, Asaka and co-workers[6] reported the first bucky gel based actuator consisting of two outer CNT composite electrodes and an inner PDVF based solid electrolyte layer. Those devices can operate at low voltages (1–4 V) and, behaving as capacitors, dissipate relatively small electrical power. When a voltage is applied to the electrodes, the cathode expands and the anode contracts, resulting in a bending motion. This is caused by the migration of ions under an electric field.[5] In the last years, thanks to developments in the device preparation process, bucky gel actuators' strain and force have been improved to the point that wearable haptic applications became possible. For this purpose, even if the actuators are inherently safe from an electrical point of view, being powered by low voltages, it would be better to avoid the direct contact of users with the actuator chemical constituents that may be potentially harmful. Moreover, an encapsulation could be useful to prevent material exposure to environmental factors, such as moisture,[11] or even more aggressive agents[12] that could alter actuator performance. In order to design safe and reliable devices, it is critical to use a proper electrical and chemical insulation barrier. Such a barrier would be beneficial even when the tactile stimulation does not imply the direct contact between the actuator and the skin, such as in the case of a Braille display.[13] Summing up, the ideal encapsulation should fulfill the three following requirements: first, it should act as a physical barrier to protect the user from getting in direct

Received: May 8, 2015
Accepted: July 1, 2015
Published: July 1, 2015

DOI: 10.1021/acsami.5b04006
ACS Appl. Mater. Interfaces 2015, 7, 15542–15550

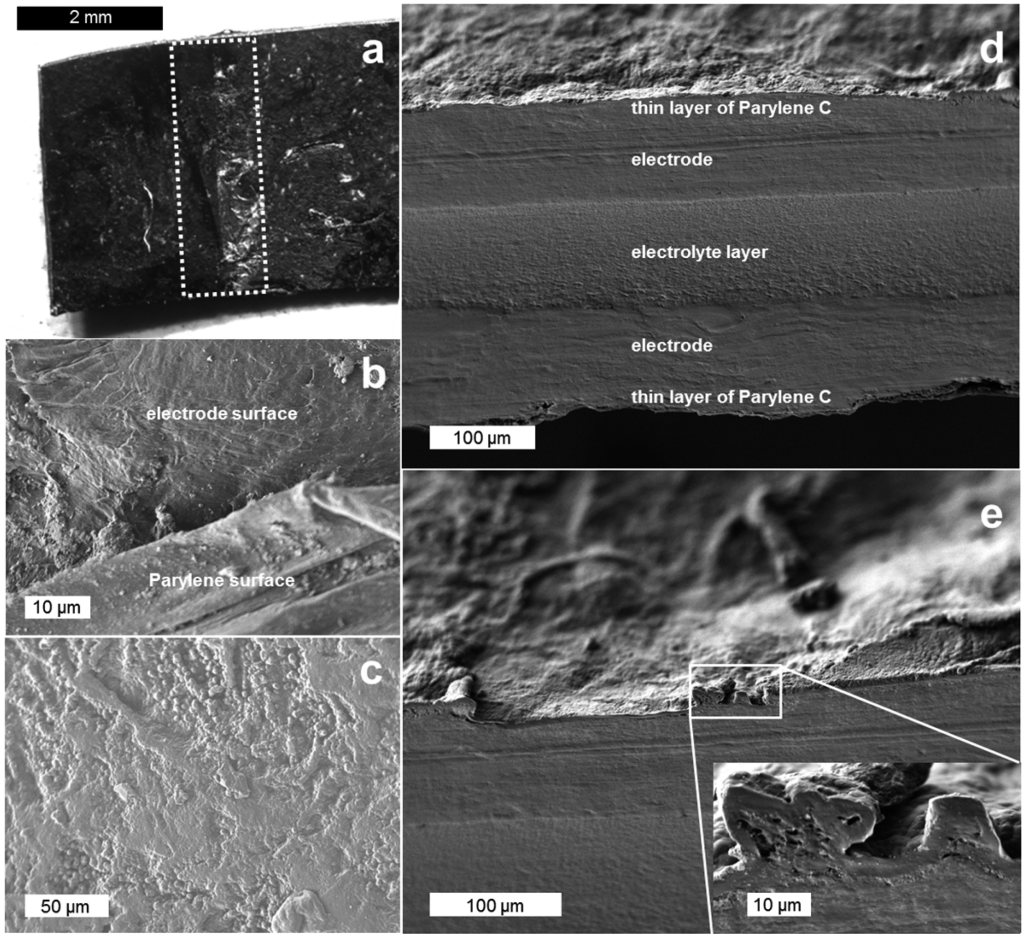

Figure 1. (a) Optical microscope picture of the coated actuator showing the boundary between coated and noncoated surface (white dotted rectangle, bare bucky gel on the left, coated one on the right). (b–e) SEM pictures of the Parylene-coated actuator: (b) border between Parylene-coated and noncoated electrode surface, (c) surface of the coated actuator, (d) cross section of the coated actuator, (e) details of the cross section showing that the Parylene coating is conformal to the bucky gel electrode surface (inset).

contact with the constituents of the actuator; second, it should provide electrical insulation; and third, it should serve as a protecting layer in order to improve the actuator lifetime and chemical resistance without affecting its performance. Herein, we present the use of Parylene C, a polymer prepared from chloro-*p*-xylylene monomer, to coat the ionic liquid–carbon nanotube composite actuators. Parylene C is a biocompatible polymer widely used for conformal coating of microelectromechanical systems (MEMS), printed circuit boards, and medical devices.[14] We chose this polymer due to its physicochemical properties such as high dielectric strength, solvent resistance, flexibility, and biological inertness.[15,16] According to the United States Administration Pharmacopeia (USP), Parylene C has the highest biocompatibility class for plastics[17,18] and it is approved to be used in implanted devices. Parylene C encapsulation of biomedical devices such as cardiac pacemakers[19] or neural interfaces has already been reported.[20] The deposition process of Parylene C allows one to obtain conformal, pinhole-free, and hydrophobic coatings at room temperature.[21] Other polymers used for encapsulating actuators such as acrylates and silicones usually produce thick layers. In contrast, the Parylene C coating process can be controlled over a wide range of film thicknesses (0.05–100 μm).[21] Thin coating layers should minimize the effect on mechanical properties that may result in a decrease of displacement and force in the final device.[22] Parylene C has already been reported as waterproof material preventing electrolyte evaporation in ionic polymer–metal composites (IPMC), although it has not yet been applied to carbon nanotube based actuators.[22] In this study, we investigated the feasibility of Parylene C coating on ionic liquid–carbon nanotube composite actuators and its effects on the performance. First, we studied the morphology of Parylene coatings using scanning electron microscopy (SEM). Then, we focused our attention on the electrochemical properties: the electronic conductivity of the electrodes, the ionic conductivity of the electrolyte layer, and the specific (gravimetric) capacitance. The quality of the coating on both bucky gel electrodes and actuators was verified by cyclic voltammetry. Finally, we evaluated the performance of the noncoated and coated actuators in terms of blocking force and strain.

2. RESULTS AND DISCUSSION

2.1. Preparation of the Actuators. The fabrication method of carbon nanotubes/ionic liquid composite actuators has been previously described.[6,23] In this work, 65–70 μm thick electrode discs were prepared from "super-growth" carbon nanotubes according to the method previously reported by Biso et al.[24] In order to obtain a reproducible and reliable electrolyte layer, we chose to make it from a commercially available PVDF membrane (Amersham Hybond SEQ, 140 μm thick, 0.2 μm

DOI: 10.1021/acsami.5b04006
ACS Appl. Mater. Interfaces 2015, 7, 15542–15550

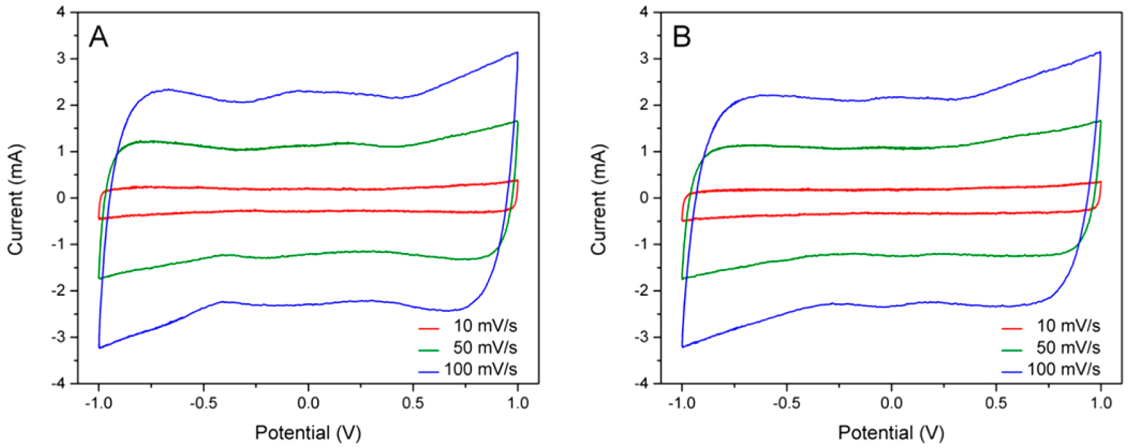

Figure 2. A comparison of voltammograms of the whole device before (A) and after (B) Parylene encapsulation. Cyclovoltammograms were recorded at three different scan rates: red, 10 mV s^{-1}; green, 50 mV s^{-1}; and blue, 100 mV s^{-1}, while potential cycled between −1 and 1 V.

pore size). The membrane was soaked in 1-butyl-3-methyl-imidazolium tetrafluoroborate (BMIM[BF_4]). After removing the excess BMIM[BF_4], the mass of the membrane was increased by 350%, suggesting that the pores are effectively filled with ionic liquid, while the thickness and the diameter were increased by 2% and 1.4%, respectively. The uptake of ionic liquid by the PVDF membrane was acknowledged by FTIR (see Figure S1 in the Supporting Information). The actuators were prepared by hot pressing the electrolyte layer in between two bucky gel electrodes. The thickness of the electrolyte layer, after the lamination, was reduced to 110 μm. Finally, the actuators were coated by a thin layer of approximately 2 μm of Parylene C, as described in the Experimental Section. In order to preserve an electrical contact, we masked one of the actuator ends by polyimide tape.

2.2. Microscopic Characterization. To characterize the microstructure of the Parylene C coating, we used both optical and scanning electron microscopy. Figure 1a shows an optical micrograph of the boundary between the coated and the noncoated actuator surface, while Figure 1b is a SEM picture of the same area: the continuous film created by the deposited Parylene can be distinguished from the noncoated bucky gel. The thin Parylene C layer is not perfectly smooth (Figure 1c) as it copies the surface features of the bucky gel layer. The cross section of the coated actuator (Figure 1d) reveals the actuator structure: the central layer is the electrolyte, from which we can distinguish the two adjacent carbon nanotubes based electrodes, and the outermost layers are Parylene C thin films. All the layers appear seamlessly connected, meaning that the lamination by hot press and the Parylene deposition were both successful. A close-up of the boundary between the bucky gel and the Parylene coating (Figure 1e) confirms that the coating is conformal—its thickness does not change on bumps or hollows—proving the successful condensation of the coating from the chemical vapor phase onto the bucky gel. In addition, no cracks or pinholes can be observed.

2.3. Electrochemical Properties of the Electrode and the Electrolyte Layer. Prior to the electromechanical characterization, we investigated the electrochemical properties of the carbon nanotube based electrodes and of their corresponding actuators before and after coating. The electronic conductivity of the electrodes measured using the four-point probe method is 24.6 S cm^{-1}, which is of the same order of magnitude as conductivities reported for similar electrodes by Sugino et al.[25] The ionic conductivity of the electrolyte layer was measured just before assembling actuators and was found to be 2.0×10^{-3} S cm^{-1}. This value surpasses by 1 order of magnitude the previously reported conductivity of 5.6×10^{-4} S cm^{-1} by Biso and Ricci[9] (electrolyte obtained by casting a mixture of PVDF, BMIM[BF_4] in tetrahydrofuran) and of 3.1×10^{-4} S cm^{-1} reported by Takeuchi et al.[26] (for a casted electrolyte layer using a solution of PVDF-HFP, BMIM[BF_4], propylene carbonate, and 4-methyl-2-pentanone). To evaluate the electric double-layer capacitance, we performed cyclic voltammetry on the actuator using a two-electrode configuration at room temperature. The voltage was applied between the two carbon nanotube composite electrodes and was cycled from −1 to 1 V. The device behaved as a supercapacitor[27] at all tested scan rates (Figure 2). The presented cyclovoltammograms exhibit no redox peaks. Similar results have previously been reported for CNT paper electrodes which were cycled in ionic liquids.[28] Moreover, when the potential gradient was reversed, the current quickly reaches a steady state, due to the low electrolyte resistance, suggesting a fast and efficient charging of the actuator. The voltammograms of the actuators prior to (Figure 2A) and after (Figure 2B) coating are almost identical, indicating the preservation of the electrochemical properties. We evaluated the capacitance of the bucky gel actuator as

$$C = \frac{I_p}{V_s} \tag{1}$$

where C is the capacitance of the device, I_p is the peak-to-peak value of the current at open-circuit potential measured by cyclic voltammetry, and V_s is the scan rate. Since the electrical model of the actuator can be represented by a supercapacitor consisting of two capacitors and a resistor in series and assuming that the electrodes are identical in mass, thickness, and size, with equal dispersion of carbon nanotubes in the polymeric matrix, the specific (gravimetric) capacitance can be calculated as follows[28]

$$C_{SP} = 4\frac{C}{m_{CNT}} \tag{2}$$

where C_{SP} is the specific capacitance of the single electric double layer and m_{CNT} is the mass of carbon nanotubes in the two electrodes of the actuator. The current values were

DOI: 10.1021/acsami.5b04006
ACS Appl. Mater. Interfaces 2015, 7, 15542−15550

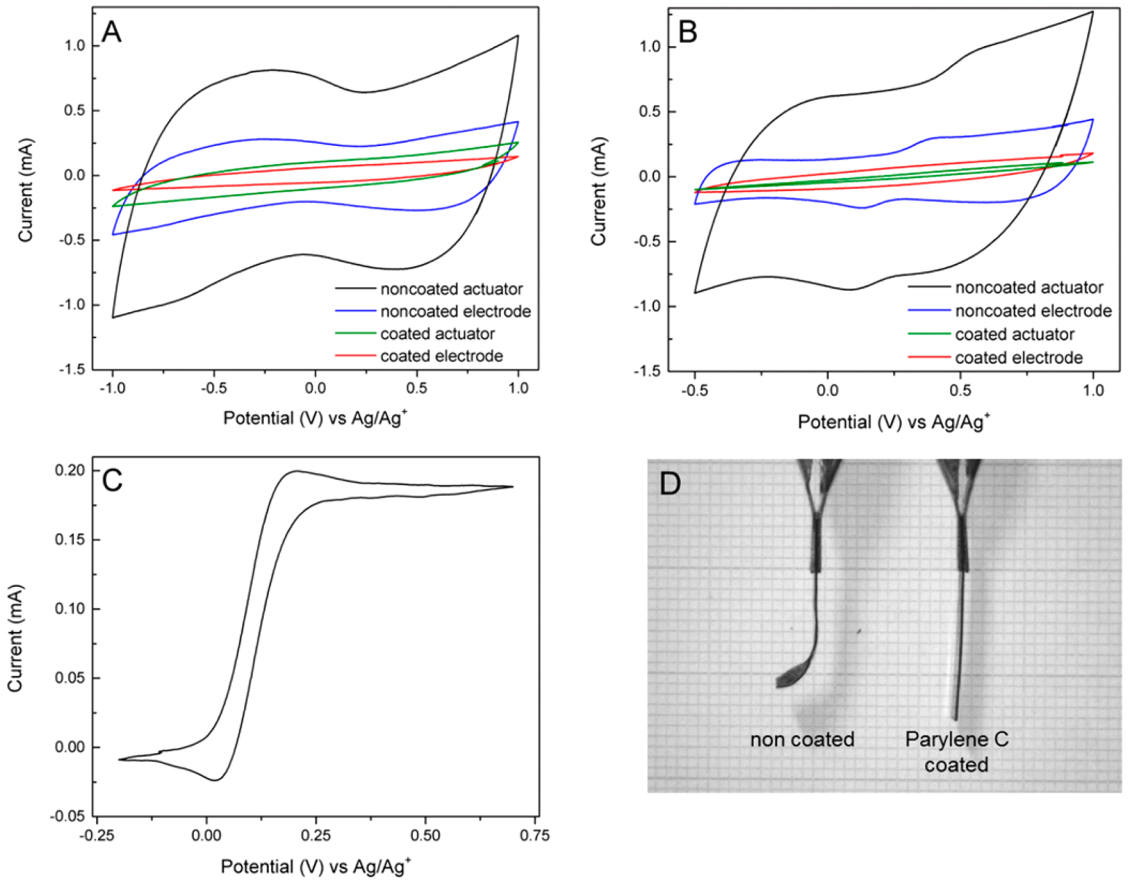

Figure 3. Cyclovoltammograms (scan rate = 10 mV s^{-1}). Black lines: bucky gel actuator; blue lines: bucky gel electrode thin film; green lines: Parylene-coated actuator; red lines: Parylene-coated electrode. Voltammograms obtained (A) before adding ferrocene and (B) after addition of ferrocene. (C) Cyclic voltammogram of a ferrocene solution under the same conditions. (D) Comparison between the noncoated and coated actuator after immersion in 2-propanol, no voltage applied.

determined for two scan rates, 10 and 100 mV s^{-1}. The calculated specific capacitances of the single double layer before coating were 93.7 F g^{-1} at 10 mV s^{-1} and 87.3 F g^{-1} at 100 mV s^{-1}. After coating, the values did not change significantly as we obtained 92.4 and 85.5 F g^{-1} for 10 and 100 mV s^{-1}, respectively. These values are approximately 2 times higher than the electrical double-layer capacitance values reported for the same actuator configuration using "super-growth" single-walled carbon nanotubes (SWCNTs) or high-purity HiPco SWCNTs (45 F g^{-1}).[8,26] We can conclude that Parylene coating does not affect significantly the electrochemical properties of the actuators.

2.4. Electrochemical Assessment of Parylene Coating Insulation Properties. We validated the quality of the Parylene coating by cyclic voltammetry as it allows us to screen a large area of the coating for cracks and leakage at the same time. We have used a three-electrode electrochemical cell configuration controlled by a potentiostat to carry out the experiment. The device under test—either single electrodes or whole actuators, both coated and noncoated—was connected as working electrode (WE) and held in position by a gold-plated clamp. The counter electrode (CE) was a platinum mesh, and we used a thin Ag strip as pseudo reference (REF). The electrolyte solution consisted of 0.1 M tetrabutylammonium hexafluorophosphate (TBA[PF_6]) in propylene carbonate (PC). To determine whether Parylene coating is an appropriate insulator or not, we recorded the cyclovoltammograms before (scan rate = 10 mV s^{-1}, potential cycling from −1 to 1 V) and after (scan rate = 10 mV s^{-1}, potential cycling from −0.5 to 1 V) adding ferrocene to the electrochemical cell. Upon addition of ferrocene, if a current flows, a reversible one-electron oxidation process of ferrocene (Fc) to ferrocenium (Fc^+) should occur at very low voltages. Typically, we added 2−3 mg of ferrocene to the electrolyte solution. Figure 3A,B shows the voltammograms of four different cases—noncoated actuator, coated actuator, noncoated electrode, and coated electrode—both without and with ferrocene. We observed, for both noncoated electrode and actuator, characteristic features around 0.5 and −0.1 V, respectively. These can be related to the oxidation−reduction peaks of the ferrocene (see Figure 3B). Cyclovoltammograms of coated actuators and electrodes exhibit no oxidation/reduction peaks due to the electrical insulation granted by the Parylene encapsulation. During the measurements, we also observed a difference in wetting of the actuators by propylene carbonate between coated and non-coated samples. Noncoated samples were quickly wetted by the solvent along the length, from the immersed part to the top part. Coated actuators and electrodes were wetted only at the part which was immersed in the solvent. Thus, in the latest case, no capillary uptake effect was observed. Surprisingly, it is worth mentioning that we observed a drastic deformation of the noncoated samples after rinsing with 2-propanol. In Figure 3D, the sample on the left is not protected by Parylene coating and does not maintain its original shape after being wetted with 2-propanol, contrary to a coated sample on the right. Needless to say, this effect was not observed for Parylene-coated

DOI: 10.1021/acsami.5b04006
ACS Appl. Mater. Interfaces 2015, 7, 15542−15550

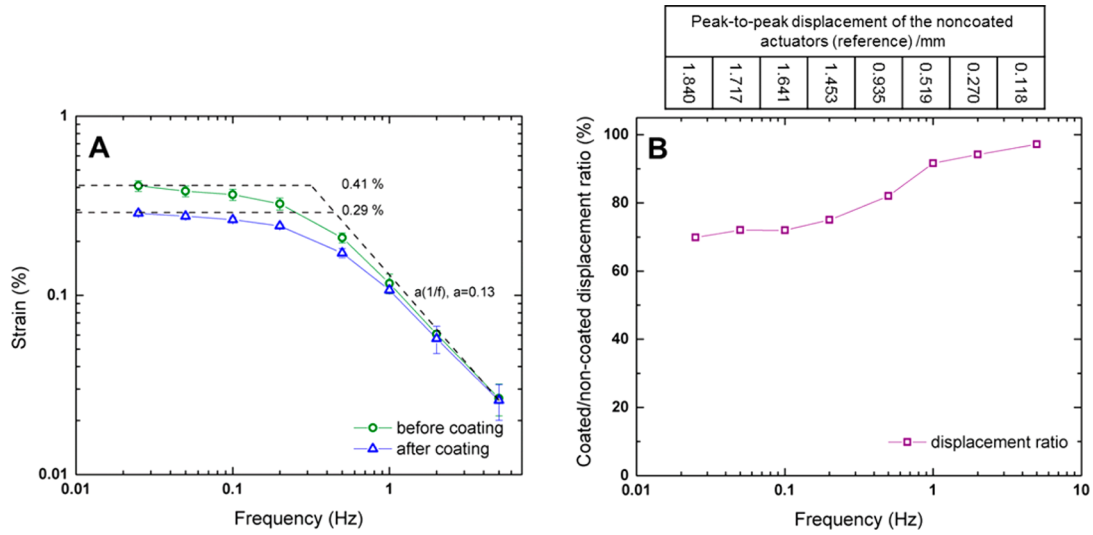

Figure 4. (A) Calculated values of the average strain from peak-to-peak displacement measured before and after Parylene coating as a function of frequency (free length L = 15 mm); log−log representation. The error bars are standard deviations of the measurement. (B) Displacement of the coated actuators expressed as a percentage of the average displacement of the same actuators before Parylene encapsulation (in the table).

actuators. In addition, we investigated protective properties of the Parylene C by immersing coated and noncoated actuators in ultrapure water for 12 h at room temperature. Then, the actuators were dried under vacuum or at atmospheric pressure. Once again, the noncoated actuators were damaged, while Parylene C-coated actuators preserved their original shape (see Figure S4 in the Supporting Information).

2.5. Performance Evaluation. Once we assessed the effectiveness of the Parylene coating, we focused our attention on evaluating the resulting actuators' performances. We characterize each actuator in terms of displacement and blocking force while applying ±1.75 V square-wave potential in open air and at room temperature on the very same samples before and after coating at the free length of 15 mm. The peak-to-peak displacement was measured for frequencies ranging from 25 mHz to 5 Hz in order to investigate conditions when the charge is applied long enough to reach the actuator's steady state as well as for a short charging time. As mentioned earlier, an electrical model of the actuator can be represented by a supercapacitor consisting of two capacitors and a resistor in series. At lower frequencies, due to the longer charging time, more charge is stored in the electrical double layers (see Figure S5 in the Supporting Information). The bucky gel actuators require that the voltage is applied for a certain time in order to be fully charged (capacitive double-layer charging) and to reach maximum displacement. Indeed, the displacement becomes higher when the voltage is applied for longer times (i.e., at lower frequencies). The strain difference ε between two composite electrode layers can be calculated from the displacement according to the following equation

$$\varepsilon = \frac{2Dt}{L^2 + D^2} \tag{3}$$

where D is the peak-to-peak displacement, t is the thickness of the actuator, and L is its free length (i.e., the distance between the end of the clamp and the actual position of the displacement meter laser spot). The strain difference, as a function of frequency, computed for the actuators before and after Parylene C coating, is reported in Figure 4A. In both conditions, the strain is almost constant at frequencies lower than 0.2 Hz, suggesting that the devices are fully charged. However, the displacement of coated actuators is reduced by 20−30% (Figure 4B). On the contrary, at frequencies above 0.5 Hz, the strain of both coated and noncoated samples decreases more or less as $1/f$ and the displacement is nearly unaffected by the coating. The strain reproducibility among the samples is higher below 0.2 Hz. Its standard deviation varies from 6.5% to 7.8% for noncoated actuators and from 2.1% to 3.4% for the Parylene-coated. For the higher frequency range, the variation became higher—from 6% at 0.5 Hz up to around 20% at 5 Hz—for both coated and noncoated actuators. Since the electrochemical properties of the actuators are unaffected by the coating, the changes in the displacement output can be correlated to the difference in mechanical properties.

The actuation features can be better evaluated through an elastic model[29] that defines the geometry-independent generated strain α as a function of the displacement

$$\alpha = \frac{EI/R}{E_1 b t_1 (t_1 + t_2)} \tag{4}$$

where EI is the flexural stiffness and R the radius of curvature of the actuator, b is the actuator width, E_1 is the Young's modulus of the bucky gel layer, and t_1 and t_2 are the thicknesses of the electrodes and of the electrolyte, respectively. The resulting value of α, 8.5×10^{-4}, is in agreement with previous studies on similar actuators.[30] In the case of coated actuators, the modified stiffness EI^* can be calculated by adding to the original stiffness the contribution from the coating

$$EI^* = EI + \frac{E_p b((t + 2t_c)^3 - t^3)}{12} \tag{5}$$

E_p is the Young's modulus of Parylene C, b is the actuator width, and t and t_c are the original thickness of the actuator ($2t_1 + t_2$) and the coating thickness, respectively. The ratio between EI and EI^* gives an estimation of the strain decrease caused by the coating. The strain loss as a function of the coating thickness follows a third-root dependence (see Figure S6 in the Supporting Information). Despite the low coating thickness, its contribution to the flexural stiffness is not negligible, increasing it by 25% as compared to the initial value. This is due to the

DOI: 10.1021/acsami.5b04006
ACS Appl. Mater. Interfaces 2015, 7, 15542−15550

larger Young's modulus of the Parylene C (2.5 GPa as measured by nanoindentation) with respect to the one of bucky gels and is furthest from the neutral axis. The changes in the flexural stiffness due to the Parylene coating were already reported by Rizzi et al. for encapsulated artificial hair cell.[31] In the higher frequency range (1−5 Hz), the actuator deflection is relatively small and the effect of the increased flexural stiffness is negligible, if compared to the standard deviation of the displacement measurement, explaining the reduced impact of the coating.

Finally, we measured the blocking force for a frequency range from 0.05 to 1 Hz (see Figure 5). The generated force is unaffected by the coating regardless of the frequency. A similar behavior was already observed by Kim et al. for Parylene-coated IPMC actuators, but the authors did not address the origin of the actuator force preservation.[22] Applying again the elastic mechanical model, the blocking force can be expressed as follows

$$F = \frac{\alpha E_1 b t_1 (t_1 + t_2)}{L} \quad (6)$$

The flexural stiffness does not take part in the equation. This is based on the assumption that no bending occurs at the actuator tip as it is blocked when the measurement is performed. Therefore, the blocking force is unaffected by the presence of the stiff coating. A maximum blocking force of ∼1.2 mN is reached at 0.1 Hz, which is consistent with a nearly fully charged device, as previously assumed from the strain vs frequency dependence (Figure 4A). The measured force of both coated and noncoated actuators is higher than the minimal force which the human finger is able to perceive (0.8 mN).[32] It is important to point out that these values were recorded at a free length of 15 mm. Since the blocking force of the tip is inversely proportional to the length of the actuator,[29] we could easily obtain higher forces by shortening the actuators. The measured output force, current, and applied voltage at 0.1 Hz for noncoated and coated actuators are shown in Figure 5b,c, respectively. Both graphs show that, after 3−4 s, the current is close to zero, which confirms both a full charging of the actuators and a very small leakage current. Interestingly, our actuators are able to generate forces of approximately 0.5 mN at 1 Hz, a relatively high frequency considering that usually generated forces for iEAP actuators are reported for a 0.05−0.1 Hz range.[23,29] The decrease of the displacement and the preservation of the blocking force is consistent with a simple model based on an isotropic elastic behavior of a composite material.

Taking into account practical applications, we further assessed the durability of the coated actuator following procedures similar to those reported in the literature.[33,34] The actuator displacement was monitored for 4 h while applying a 0.1 Hz sinusoidal wave of the same potential as for the displacement and force characterization (±1.75 V). We found that the performance (peak-to-peak displacement) of the actuator was maintained throughout the experiment (see Figure S7 in the Supporting Information). Moreover, all the five layers constituting the actuator were still well connected. Concerning the long-term stability, we evaluated the performances of the coated actuator after more than 4 months of storage. We did not notice any significant loss in displacement when a ± 1.75 V square wave was applied. At 25 mHz, a maximum displacement of 1.692 mm was obtained, which corresponds to 95% of the displacement before the storage period. In addition, the cyclic voltammetry results of that sample remained unchanged (Figure S8 in the Supporting Information), suggesting the preservation of the double-layer capacitance.

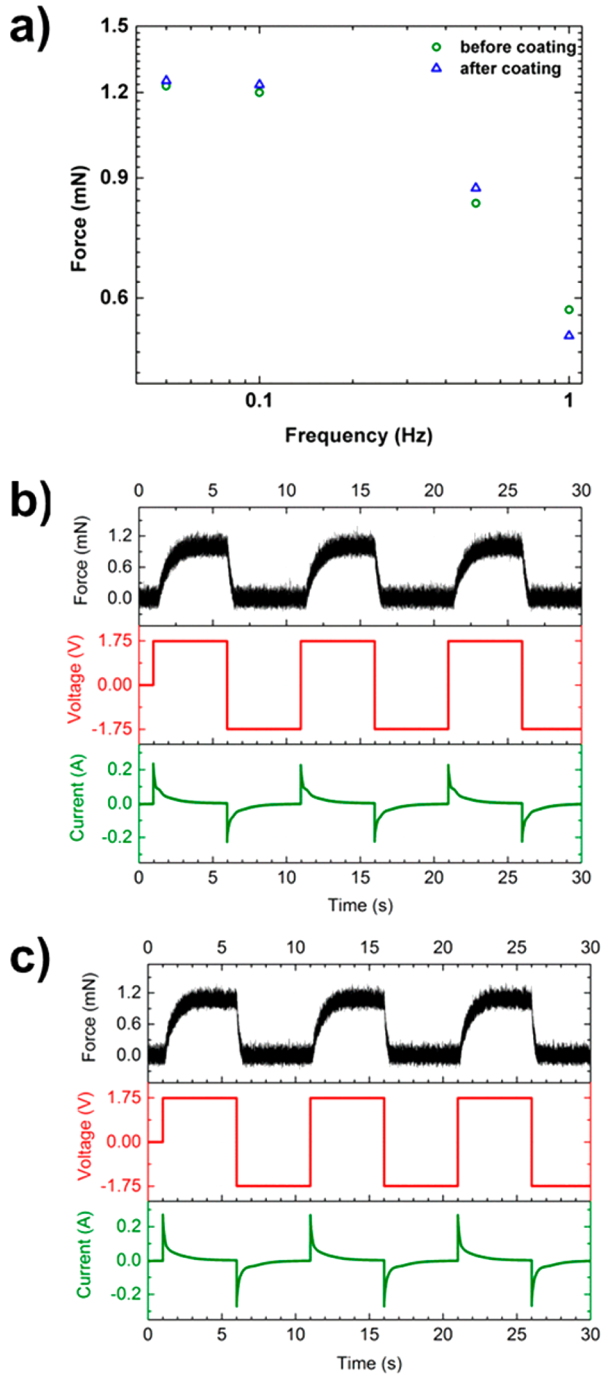

Figure 5. (a) Force output as a function of frequency. (b) Force−voltage−current response for noncoated actuator at 0.1 Hz. (c) Force−voltage−current response after coating at 0.1 Hz. Force measurements were carried out under ±1.75 V square-wave potential.

3. CONCLUSION

We demonstrated the successful encapsulation of ionic liquid−carbon nanotube composite actuators by a Parylene C coating and that this approach is appropriate for bucky gel actuators. Positive results, following the electrochemical validation for both actuators and electrodes, suggest its feasibility for other

DOI: 10.1021/acsami.5b04006
ACS Appl. Mater. Interfaces 2015, 7, 15542−15550

kinds of soft actuators based on carbon nanotubes. The actuators coated by a thin layer of Parylene C preserve the generated force, and the displacement reduction at low frequencies (0.025−0.2 Hz) is not substantial. At higher frequencies (1−5 Hz), which are more appropriate for haptic devices, both blocking force and displacement are unaffected by the Parylene coating. We demonstrated that this coating effectively protects the device from external agents such as water and alcohols, disclosing the possibility of their use in environments such as water solutions or body fluids. Because of Parylene C biocompatibility, the encapsulated actuators are safe to touch and can be used in contact with human skin and in biomedical applications in direct contact with tissues and physiological fluids. Considering the ease of preparation of this type of carbon nanotube actuators, the Parylene coating opens the door to the production of a variety of lightweight devices for direct tactile stimulation without the need to interpose further mechanical elements.

4. EXPERIMENTAL SECTION

4.1. Preparation of Electrodes. A 246 mg portion of 1-butyl-3-methylimidazolium tetrafluoroborate (43 wt %, Sigma-Aldrich) was added to 88 mg of single-walled carbon nanotubes (15 wt %, HT "super-growth" provided by the Nanotube Research Center of the National Institute of Advanced Industrial Science and Technology (AIST), Japan) and to 239 mg of polyvinylidene difluoride (42 wt %, PVDF, M_w = 534 000, Sigma-Aldrich). Then, 15 mL of *N*,*N*-dimethylacetamide (Sigma-Aldrich) was added, and the mixture was stirred at the room temperature for 1 h. Then, the mixture was probe-sonicated at 39 W for 45 min (4 s on/2 s off) in order to create a gel, which was later casted on a glass mold and dried at 80 °C until complete evaporation of the solvent. Finally, discs were cut out (diameter = 28 mm) and their thickness was reduced by hot pressing (Specac Atlas T8 Power Press, temperature = 215 °C, applied weight = 1 ton, few seconds, 50 μm spacer thickness).

4.2. Preparation of the Electrolyte Layer. PVDF discs (diameter = 28 mm and thickness = 140−143 μm) were cut out from a membrane sheet (Amersham Hybond SEQ, 0.2 μm pore size, PVDF blotting membrane). Then, 800 mg of 1-butyl-3-methylimidazolium tetrafluoroborate was dropped on the membrane in order to fully cover it. Discs were left overnight in a glass Petri dish closed with Parafilm. The resulting electrolyte layer was dried under vacuum (BÜCHI b-585 glass oven) for 60 h at 60 °C in order to remove any presence of humidity. Prior to the actuators assembling and testing, the electrolyte layer was kept in a closed glass Petri dish.

4.3. Assembly of Ionic Liquid−Carbon Nanotube Based Actuators. The final device was obtained by hot press lamination (Specac Atlas T8 Power Press) of three layers (each one of 28 mm): two outer layers (electrodes) that were previously pressed and the inner electrolyte layer. Then, actuators (with the following dimensions: length = 20 mm, width = 4 mm, thickness = 253 μm) were cut out and characterized both before and after Parylene coating. We used a lamination procedure similar to the one previously reported by us.[24] The following press parameters were used: set up pressure = 1 T, 1 h of pressing time, T = 130 °C, spacer thickness = 250 μm.

4.4. Parylene Coating. The Parylene C layer was deposited on the actuators by chemical vapor deposition using an SCS Labcoter 2 Parylene Deposition System. Prior to the deposition, Silquest A-174 primer was evaporated and created a monolayer on every surface. Next, DPX-C Parylene C dimer was pyrolized into reactive monomer at a temperature around 680 °C. The monomer then flowed to the deposition chamber and polymerized on the actuators. During the whole process, the temperature of the sample in the deposition chamber is close to room temperature.

4.5. Scanning Electron Microscopy (SEM). Microphotographs were taken using a high-resolution scanning electron microscope JEOL JSM-7500FA. Acceleration voltage: 2 kV; detector: lower secondary electron detector (LEI).

4.6. Optical Microscopy. An optical microscope, Leica Z16 APO, with a Leica DFC295 digital camera was used.

4.7. Physical Properties. The thickness of the electrodes and electrolyte layers after hot pressing as well as laminated actuators was measured at three different points using a Mitutoyo Absolute Digimatic Micrometer Series 227 (accuracy of 2 μm); then, average values were used. In order to calculate the density, each device was weighed on an analytical balance with a resolution of 1×10^{-5} g (Mettler Toledo XS205). The thickness of the electrolyte layer after lamination was assessed by comparing the total actuator thickness before and after lamination, based on the safe assumption that, due to the significantly lower Young's modulus of the electrolyte layer, it will be the only one to undergo thickness reduction. Young's modulus of the electrolyte layer is typically 33 ± 4 MPa and 530 ± 76 MPa for the bucky gel electrode.

4.8. FTIR Spectra. Both pristine PVDF membrane and electrolyte layers prepared by soaking the membrane in BMIM[BF_4] were characterized using fourier transform infrared spectroscopy. Spectra were recorded at room temperature using a Bruker V70 spectrometer in the 600−4000 cm^{-1} range with a resolution of 4 cm^{-1}.

4.9. Electronic Conductivity. Electronic conductivity of the electrodes was evaluated based on four probe measurements using the following equation

$$\sigma = \frac{1}{\rho} = \frac{L}{R\omega t} \tag{7}$$

where σ is the conductivity ($S \cdot cm^{-1}$), ρ is the resistivity ($\Omega \cdot cm^{-1}$), L is the distance between two inner sense wires (0.1 cm), and ω and t are the width and the thickness of the samples in cm, respectively. Measurements were carried out using a Keithley 2612 source meter. We measured the voltage when a current ramp wave from −0.5 to 0.5 mA (20 points) was applied. Resistance (R) was calculated from the $I-V$ curve using the following equation:

$$R = \frac{\frac{V_1}{-0.5\text{ mA}} + \frac{V_2}{-0.45\text{ mA}} + \frac{V_{19}}{0.5\text{ mA}} + \frac{V_{20}}{0.45\text{ mA}}}{4} \tag{8}$$

4.10. Ionic Conductivity. Ionic conductivity of the electrolyte layer was measured by electrochemical impedance spectroscopy (EIS) in a two-electrode configuration at open-circuit voltage from 2 kHz to 2 MHz under 100 mV AC perturbation using an Agilent E4980A precision LCR meter. Measurements were carried out at room temperature.

4.11. Cyclic Voltammetry. Cyclic voltammetry of the coated and noncoated actuators was recorded in air at the room temperature with a computer-controlled AMEL 2549 potentiostat in a two-electrode configuration. The potential was cycled between −1 and 1 V with the following scan rates: 10, 50, and 100 mV s^{-1}. Actuator electrodes were clamped using gold-plated Kelvin clamps.

4.12. Parylene Coating Validation by Cyclic Voltammetry. To validate Parylene coating quality, we carried out cyclic voltammetry at room temperature under a nitrogen atmosphere with a computer-controlled AMEL 2549 potentiostat in a three-electrode configuration. The potential was cycled from −1 to 1 V at a scan rate of 10 mV s^{-1}. In the case of coated samples, the potential was cycled from −0.5 to 1 V. The samples under test—a strip of noncoated or coated carbon nanotubes based electrode or assembled actuator—were connected as the working electrode (WE), held in position by gold-plated Kelvin clamps. The counter electrode (CE) was a platinum mesh, and the pseudo-reference electrode (REF) was a thin Ag strip. The electrochemical cell was dried for 10 min in an oven at 60 °C. Propylene carbonate (PC) was sparged with nitrogen for 20 min. Then, the electrolyte (0.1 M TBA[PF_6] in PC) was added to the cell and stirred. Before measuring the samples, we carried out cyclic voltammetry of the ferrocene solution using a Pt mesh as a WE (scan rate = 10 mV s^{-1}, potential range from −0.2 to 0.7 V). Typically, 2−3 mg of ferrocene was added to the electrolyte.

4.13. Displacement. Displacement was measured using a micro-epsilon ILD 1700-50 laser sensor (3 μm resolution, maximum sampling rate = 1.25 kHz).

DOI: 10.1021/acsami.5b04006
ACS Appl. Mater. Interfaces 2015, 7, 15542−15550

4.14. Force Measurements. An Aurora Scientific dual-mode lever arm system model 300C with a signal interface model 604A was employed to measure the force (with a resolution of 0.3 mN).

4.15. Mechanical Properties Characterization. Young's moduli of single electrodes and electrolytes were measured through uniaxial tensile tests on a 3365 dual column Instron universal testing machine. Samples were cut from the pressed discs in strips of about 28×4 mm^2 and tested with the rate of 2 mm min^{-1}. Young's modulus was calculated from the resulting stress strain curves. Values were averaged from at least 3 specimens per sample. Young's modulus of the Parylene C coating was measured by nanoindentation on a layer purposely deposited on a glass slide, with the same coating conditions as actuators. Twenty indentation tests were performed on a CSM UHNT nanoindenter equipped with a Berkovich tip, under the maximum load of 100 μN, and the Young's modulus was calculated with the Oliver and Pharr method.

■ ASSOCIATED CONTENT

Supporting Information

FTIR spectra, SEM picture of the PVDF membrane, Nyquist plot of the electrolyte layer, calculated applied charge, results of the actuators exposure to water, experimental and theoretical strain for different coating thicknesses, durability measurement, and cyclovoltammograms of the actuator before and after long-term storage. The Supporting Information is available free of charge on the ACS Publications website at DOI: 10.1021/acsami.5b04006.

■ AUTHOR INFORMATION

Corresponding Author

*E-mail: grzegorz.bubak@iit.it.

Author Contributions

The manuscript was written through contributions of all authors. All authors have given approval to the final version of the manuscript.

Notes

The authors declare no competing financial interest

■ ABBREVIATIONS

iEAP, ionic electroactive polymer
CNTs, carbon nanotubes
PVDF, polyvinylidene difluoride
PVDF-HFP, poly(vinylidene fluoride-*co*-hexafluoropropylene)
BMIM[BF_4], 1-butyl-3-methylimidazolium tetrafluoroborate
TBA[PF_6], tetrabutylammonium hexafluorophosphate
PC, propylene carbonate
SWCNTs, single-walled carbon nanotubes

■ REFERENCES

(1) Kim, K. J.; Tadokoro, S. *Electroactive Polymers for Robotic Applications: Artificial Muscles and Sensors*; Springer-Verlag: London, U.K., 2007.
(2) Mirfakhrai, T.; Madden, J. D. W.; Baughman, R. H. Polymer Artificial Muscles. *Mater. Today* **2007**, *10*, 30−38.
(3) Bar-Cohen, Y. In *Electroactive Polymer (EAP) Actuators as Artificial Muscles*; Bar-Cohen, Y., Ed.; SPIE Press: Bellingham, WA, 2004; Chapter 1, pp 3−42.
(4) Tiwari, R.; Garcia, E. The State of Understanding of Ionic Polymer Metal Composite Architecture: a Review. *Smart Mater. Struct.* **2011**, *20*, 083001.
(5) Kong, L.; Chen, W. Carbon Nanotube and Graphene-Based Bioinspired Electrochemical Actuators. *Adv. Mater.* **2014**, *26*, 1025−1043.
(6) Fukushima, T.; Asaka, K.; Kosaka, A.; Aida, T. Fully Plastic Actuator Through Layer-by-Layer Casting with Ionic-Liquid-Based Bucky Gel. *Angew. Chem., Int. Ed.* **2005**, *44*, 2410−2413.
(7) Fukushima, T.; Kosaka, A.; Ishimura, Y.; Yamamoto, T.; Takigawa, T.; Ishii, N.; Aida, T. Molecular Ordering of Organic Molten Salts Triggered by Single-Walled Carbon Nanotubes. *Science* **2003**, *300*, 2072−2074.
(8) Mukai, K.; Asaka, K.; Sugino, T.; Kiyohara, K.; Takeuchi, I.; Terasawa, N.; Futaba, D. N.; Hata, K.; Fukushima, T.; Aida, T. Highly Conductive Sheets from Millimeter-Long Single-Walled Carbon Nanotubes and Ionic Liquids: Application to Fast-Moving, Low-Voltage Electromechanical Actuators Operable in Air. *Adv. Mater.* **2009**, *21*, 1582−1585.
(9) Biso, M.; Ricci, D. Multi-walled Carbon Nanotubes Plastic Actuator. *Phys. Status Solidi B* **2009**, *246*, 2820−2823.
(10) Terasawa, N.; Ono, N.; Hayakawa, Y.; Mukai, K.; Koga, T.; Higashi, N.; Asaka, K. Effect of Hexafluoropropylene on the Performance of Poly(vinylidene fluoride) Polymer Actuators Based on Single-Walled Carbon Nanotube−Ionic Liquid Gel. *Sens. Actuators, B* **2011**, *160*, 161−167.
(11) Must, I.; Vunder, V.; Kaasik, F.; Põldsalu, I.; Johanson, U.; Punning, A.; Aabloo, A. Ionic Liquid-Based Actuators Working in Air: The Effect of Ambient Humidity. *Sens. Actuators, B* **2014**, *202*, 114−122.
(12) Punning, A.; Kim, K. J.; Viljar, P.; Vidal, F.; Plesse, C.; Festin, N.; Maziz, A.; Asaka, K.; Sugino, T.; Alici, G.; Spinks, G.; Wallace, G.; Must, I.; Põldsalu, I.; Vunder, V.; Temmer, R.; Kruusamäe, K.; Torop, J.; Kaasik, F.; Rinne, P.; Johanson, U.; Peikolainen, A.-L.; Tamm, T.; Aabloo, A. Ionic Electroactive Polymer Artificial Muscles in Space Applications. *Sci. Rep.* **2014**, *4*, 6913.
(13) Fukuda, K.; Sekitani, T.; Zschieschang, U.; Klauk, H.; Kuribara, K.; Yokota, T.; Sugino, T.; Asaka, K.; Ikeda, M.; Kuwabara, H.; Yamamoto, T.; Takimiya, K.; Fukushima, T.; Aida, T.; Takamiya, M.; Sakurai, T.; Someya, T. A 4 V Operation, Flexible Braille Display Using Organic Transistors, Carbon Nanotube Actuators, and Organic Static Random-Access Memory. *Adv. Funct. Mater.* **2011**, *21*, 4019−4027.
(14) Hassler, C.; Boretius, T.; Stieglitz, T. Polymers for Neural Implants. *J. Polym. Sci., Part B: Polym. Phys.* **2011**, *49*, 18−33.
(15) Trantidou, T.; Tariq, M.; Terracciano, C. M.; Toumazou, C.; Prodromakis, T. Parylene C-Based Flexible Electronics for pH Monitoring Applications. *Sensors* **2014**, *14*, 11629−11639.
(16) Senkevich, J. J.; Desu, S. B. Morphology of Poly (chloro-p-xylylene) CVD Thin Films. *Polymer* **1999**, *40*, 5751−5759.
(17) Rodger, D. C.; Fong, A. J.; Li, W.; Ameri, H.; Ahuja, A. K.; Gutierrez, C.; Lavrov, I.; Zhong, H.; Menon, P. R.; Meng, E.; Burdick, J. W.; Roy, R. R.; Edgerton, V. R.; Weiland, J. D.; Humayun, M. S.; Tai, Y.-C. Flexible Parylene-Based Multielectrode Array Technology for High-Density Neural Stimulation and Recording. *Sens. Actuators, B* **2008**, *132*, 449−460.
(18) Seymour, J. P.; Elkasabi, Y. M.; Chen, H.-Y.; Lahann, J.; Kipke, D. R. The Insulation Performance of Reactive Parylene Films in Implantable Electronic Devices. *Biomaterials* **2009**, *30*, 6158−6167.
(19) Iguchi, N.; Kasanuki, H.; Matsuda, N.; Shoda, M.; Ohnishi, S.; Hosoda, S. Contact Sensitivity to Polychloroparaxylene-Coated Cardiac Pacemaker. *Pacing Clin. Electrophysiol.* **1997**, *20*, 372−373.
(20) Hsu, J.-M.; Rieth, L.; Normann, R. A.; Tathireddy, P.; Solzbacher, F. Encapsulation of an Integrated Neural Interface Device With Parylene C. *IEEE Trans. Biomed. Eng.* **2009**, *56* (1), 23−29.
(21) Beach, W. F. In *Coatings Technology Handbook*, 3rd ed.; Tracton, A. A., Ed.; CRC Press: Boca Raton, FL, 2006; Chapter 62, p 62-1−62-3.
(22) Kim, S. J.; Lee, I. T.; Lee, H.-Y.; Kim, Y. H. Performance Improvement of an Ionic Polymer−Metal Composite Actuator by Parylene Thin Film Coating. *Smart Mater. Struct.* **2006**, *15*, 1540−1546.
(23) Mukai, K.; Asaka, K.; Kiyohara, K.; Sugino, T.; Takeuchi, I.; Fukushima, T.; Aida, T. High Performance Fully Plastic Actuator

DOI: 10.1021/acsami.5b04006
ACS Appl. Mater. Interfaces 2015, 7, 15542−15550

Based on Ionic-Liquid-Based Bucky Gel. *Electrochim. Acta* **2008**, *53*, 5555−5562.
(24) Biso, M.; Ansaldo, A.; Picardo, E.; Ricci, D. Increasing the Maximum Strain and Efficiency of Bucky Gel Actuators by Pyrrole Oxidative Polymerization on Carbon Nanotubes Dispersed in an Ionic Liquid. *Carbon* **2012**, *50*, 4506−4511.
(25) Sugino, T.; Kiyohara, K.; Takeuchi, I.; Mukai, K.; Asaka, K. Actuator Properties of the Complexes Composed by Carbon Nanotube and Ionic Liquid: the Effects of Additives. *Sens. Actuators, B* **2009**, *141*, 179−186.
(26) Takeuchi, I.; Asaka, K.; Kiyohara, K.; Sugino, T.; Terasawa, N.; Mukai, K.; Fukushima, T.; Aida, T. Electromechanical Behavior of Fully Plastic Actuators Based on Bucky Gel Containing Various Internal Ionic Liquids. *Electrochim. Acta* **2009**, *54*, 1762−1768.
(27) Béguin, F.; Presser, V.; Balducci, A.; Frackowiak, E. Carbons and Electrolytes for Advanced Supercapacitors. *Adv. Mater.* **2014**, *26*, 2219−2251.
(28) Barisci, J. N.; Wallace, G. G.; MacFarlane, D. R.; Baughman, R. H. Investigation of Ionic Liquids as Electrolytes for Carbon Nanotube Electrodes. *Electrochem. Commun.* **2004**, *6* (1), 22−27.
(29) Alici, G.; Huynh, N. N. Predicting Force Output of Trilayer Polymer Actuators. *Sens. Actuators, A* **2006**, *132*, 616−625.
(30) Ceseracciu, L.; Biso, M.; Ansaldo, A.; Futaba, D. N.; Hata, K.; Barone, A. C.; Ricci, D. Mechanics and Actuation Properties of Bucky Gel-Based Electroactive Polymers. *Sens. Actuators, B* **2011**, *156*, 949−953.
(31) Rizzi, F.; Qualtieri, A.; Chambers, L. D.; Megill, W. M.; De Vittorio, M. Parylene Conformal Coating Encapsulation as a Method for Advanced Tuning of Mechanical Properties of an Artificial Hair Cell. *Soft Matter* **2013**, *9*, 2584−2588.
(32) Kern, T. A. In *Engineering Haptic Devices*; Kern, T. A., Ed.; Springer-Verlag: Berlin, Germany, 2009; Chapter 3, pp 51−52.
(33) Yun, S.-R.; Yun, G. Y.; Kim, J. H.; Chen, Y.; Kim, J. Electro-Active Paper for a Durable Biomimetic Actuator. *Smart Mater. Struct.* **2009**, *18*, 024001.
(34) Kim, J.; Jeon, J.-H.; Kim, H.-J.; Lim, H.; Oh, I.-K. Durable and Water-Floatable Ionic Polymer Actuator with Hydrophobic and Asymmetrically Laser-Scribed Reduced Graphene Oxide Paper Electrodes. *ACS Nano* **2014**, *8*, 2986−2997.

DOI: 10.1021/acsami.5b04006
ACS Appl. Mater. Interfaces 2015, 7, 15542−15550